

Direct Observation of Photoinduced Tautomerization in Single Molecules at a Metal Surface

H. Böckmann,[†] S. Liu,[†] J. Mielke,[†] S. Gawinkowski,[§] J. Waluk,^{§,||} L. Grill,^{†,‡} M. Wolf,[†] and T. Kumagai^{*,†}

[†]Department of Physical Chemistry, Fritz-Haber Institute of the Max-Planck Society, Faradayweg 4–6, 14195 Berlin, Germany

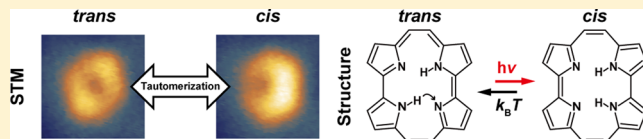
[‡]Department of Physical Chemistry, University of Graz, Heinrichstrasse 28, 8010 Graz, Austria

[§]Institute of Physical Chemistry, Polish Academy of Sciences, Kasprzaka 44/52, Warsaw 01-224, Poland

^{||}Faculty of Mathematics and Natural Sciences, College of Science, Cardinal Stefan Wyszyński University, Dewajtis 5, 01-815 Warsaw, Poland

Supporting Information

ABSTRACT: Molecular switches are of fundamental importance in nature, and light is an important stimulus to selectively drive the switching process. However, the local dynamics of a conformational change in these molecules remain far from being completely understood at the single-molecule level. Here, we report the direct observation of photoinduced tautomerization in single porphycene molecules on a Cu(111) surface by using a combination of low-temperature scanning tunneling microscopy and laser excitation in the near-infrared to ultraviolet regime. It is found that the thermodynamically stable trans configuration of porphycene can be converted to the metastable cis configuration in a unidirectional fashion by photoirradiation. The wavelength dependence of the tautomerization cross section exhibits a steep increase around 2 eV and demonstrates that excitation of the Cu d-band electrons and the resulting hot carriers play a dominant role in the photochemical process. Additionally, a pronounced isotope effect in the cross section (~ 100) is observed when the transferred hydrogen atoms are substituted with deuterium, indicating a significant contribution of zero-point energy in the reaction. Combined with the study of inelastic tunneling electron-induced tautomerization with the STM, we propose that tautomerization occurs via excitation of molecular vibrations after photoexcitation. Interestingly, the observed cross section of $\sim 10^{-19}$ cm² in the visible–ultraviolet region is much higher than that of previously studied molecular switches on a metal surface, for example, azobenzene derivatives (10^{-23} – 10^{-22} cm²). Furthermore, we examined a local environmental impact on the photoinduced tautomerization by varying molecular density on the surface and find substantial changes in the cross section and quenching of the process due to the intermolecular interaction at high density.



KEYWORDS: Molecular switch, tautomerization, photochemistry, single molecule, metal surface, scanning tunneling microscopy

Molecular switches are involved in a variety of chemical and biological processes, whose conformation and properties can be changed reversibly with external stimuli.¹ Photoexcitation is a common way to selectively drive the process whereby the reaction products, which may differ from those obtained by thermal activation, can be controlled by the excitation wavelength. Many types of photoactive molecular switches have been developed, motivated by their promising potential for future applications. Modification of surfaces with switching molecules is one application possibility, leading to “functional surfaces” that can change the morphology and functionality in response to light.² However, the carefully designed function of a molecule may be easily changed or, in the worst case, even completely disabled by the local environment, such as molecule–molecule and molecule–surface interactions. Recently, several classes of photoswitchable molecules have been investigated on various surfaces under ultrahigh vacuum conditions and the switching of individual molecules has been directly observed by using low-temperature scanning tunneling microscopy (STM).^{3–13} These studies have

revealed the significant influence from coupling of the molecule to the surface and/or to the adjacent molecules on the switching behavior. This may cause a serious problem; for instance, the isomerization cross section of self-assembled azobenzene derivatives on a metal surface ($\sim 10^{-23}$ – 10^{-22} cm²)^{4,14} is much lower compared to that in solution ($\sim 10^{-19}$ – 10^{-18} cm²). Furthermore, on a metal surface, the lifetime of excited states is extremely short (on the order of femtoseconds^{15,16}) due to rapid relaxation to the substrate, which also inhibits photochemical reactions.^{11,17} Accordingly, molecular switching that occurs at high efficiency remains a critical issue in the field.

An intriguing model of molecular switching is provided by tautomerization in porphyrin and phthalocyanine derivatives. These molecules have recently gained more attention in the field of nanoscience because of their wide variety of

Received: October 8, 2015

Revised: December 31, 2015

Published: January 21, 2016



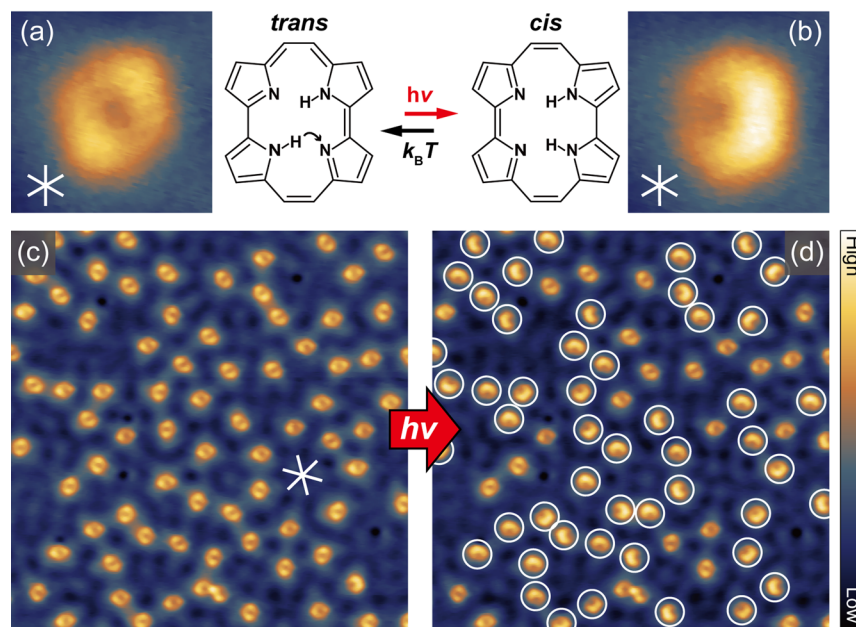


Figure 1. (a,b) STM images of a single porphycene molecule in the trans and cis configuration on Cu(111) at 5 K (size: $1.75 \times 1.75 \text{ nm}^2$, $V_{\text{bias}} = 0.1 \text{ V}$, $I_t = 0.1 \text{ nA}$). The chemical structures are displayed next to the image. The white lines in the image represent the high-symmetry axes of the surface. (c) Large-scale STM image after molecular deposition (size: $25 \times 25 \text{ nm}^2$, $V_{\text{bias}} = 0.05 \text{ V}$, $I_t = 0.05 \text{ nA}$). (d) The same area as (c) after irradiation with a 405 nm diode laser (CW, 2.7 mW) for 2 min. The switched molecules are marked by white circles. The STM tip was retracted by $\sim 2 \mu\text{m}$ from the surface during irradiation.

functionalities and self-assembly capabilities.¹⁸ Tautomerization of adsorbed naphthalocyanine,¹⁹ tetraphenylporphyrin,²⁰ and porphycene molecules^{21–24} has been investigated by using a low-temperature STM. These studies have demonstrated single-molecule switching by inelastic tunneling electrons or by thermal activation. Furthermore, the tautomerization process has been controlled by modifying the atomic environment using STM manipulation.^{22,23} However, the STM-induced excitation is extremely localized, that is, within a single molecule or to a regime within tens of nanometers from the tip for a nonlocal process^{13,22} and cannot be used for collective transformation of functionalized molecules. In this Letter, we present the first direct observation of photoinduced tautomerization in single porphycene molecules on the Cu(111) surface at 5 K.

Porphycene, a structural isomer of free-base porphyrin, is a unique model of tautomerization.²⁵ Unlike free-base porphyrin, porphycene has relatively strong H bonds within the molecular cavity,²⁶ resulting in distinctive tautomerization behavior, for example, a very fast tautomerization rate via quantum tunneling.²⁷ Additionally, better photochemical properties of porphycene in the visible region, such as higher absorption coefficients than porphyrin, may be advantageous to a photoinduced reaction.²⁸ Photoinduced tautomerization of porphycene has been studied by using polarized fluorescence spectroscopy that allows to monitor tautomerization even in a single molecule through the change of the transition dipole moment.^{29,30} In theory, porphycene has three different two-fold degenerate tautomers, defined by the position of the inner H atoms (see Supporting Information, Figure S1). Although the trans configuration is most stable in the isolated molecule, our previous studies have revealed that the relative stability of tautomers depends on the underlying surface (specifically the interaction between the non-hydrogenated N atoms within the molecule and the surface).^{22,23} On Cu(111), the trans

configuration (Figure 1a) is found to be the thermodynamically stable state, however, the trans molecule can be converted to the metastable cis(-1) configuration (Figure 1b) by inelastic tunneling electrons in the STM.²³

Here we demonstrate that the trans porphycene molecules can also be converted to the cis configuration in a unidirectional fashion by photoirradiation. Figure 1c shows a large-scale STM image of porphycene molecules on Cu(111) at 5 K. After deposition at room temperature, all molecules were found in the trans configuration on the clean terraces and were homogeneously distributed over the surface without aggregating into molecular clusters or islands. Figure 1d shows the same surface area as in Figure 1c but after exposure to a 405 nm laser, where many molecules were converted to the cis configuration. Importantly, no tautomerization was ever observed without light and below a bias voltage (V_{bias}) of 150 mV. All cis molecules can be switched back to the trans configuration by heating the surface above $\sim 35 \text{ K}$. It should be noted that the reversible cis \leftrightarrow cis tautomerization was also induced by photoirradiation, but no cis \rightarrow trans and trans \leftrightarrow trans conversion was observed. In the following, we focus on the unidirectional trans \rightarrow cis process.

The elementary excitation of photochemical processes on metal surfaces have been classified into direct absorption and substrate-mediated indirect mechanisms.^{31–35} In order to clarify the excitation mechanism behind the photoinduced tautomerization, we investigated the wavelength, power and polarization dependence of its cross section. Figure 2a shows the fraction of trans and cis molecules ($N_{\text{trans/cis}}$) with respect to the total number of molecules (N_{total}) as a function of the dosed photon number at 405 nm excitation wavelength. The evolution of $\frac{N_{\text{cis/trans}}}{N_{\text{total}}}$ follows a first-order process, and the cross section of the trans \rightarrow cis tautomerization ($\sigma_{t \rightarrow c}$) is determined by fitting the data to the rate equation

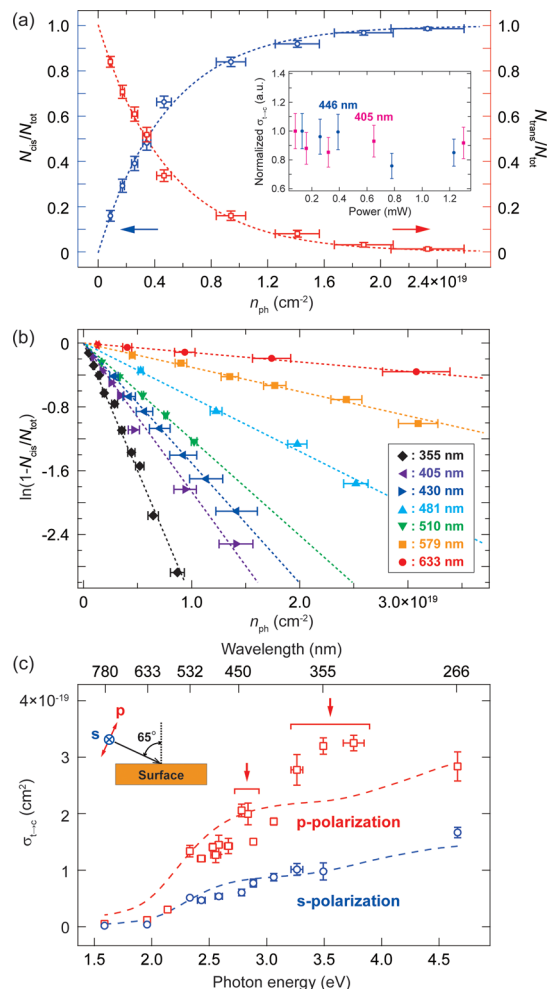


Figure 2. (a) $N_{\text{cis}}/N_{\text{tot}}$ (left axis) and $N_{\text{trans}}/N_{\text{tot}}$ (right axis) as a function of n_{ph} at 405 nm excitation wavelength (N_{total} more than 1000 were counted for each data point). The dashed curves represent the best fitted result to eq 1. The inset shows the incident power dependence of the normalized $\sigma_{\text{t}\rightarrow\text{c}}$ at 446 nm (purple) and 405 nm (blue) excitation wavelengths. (b) $\ln\left(\frac{1 - N_{\text{cis}}}{N_{\text{tot}}}\right)$ versus n_{ph} plot at various excitation wavelengths with p-polarization. The dashed lines represent the best fitted result to eq 1. (c) Wavelength (photon energy) dependence of $\sigma_{\text{t}\rightarrow\text{c}}$ measured with p- (red squares) and s-polarized light (blue squares). The geometry of the incident beam and the surface is illustrated in the upper left. The red arrows indicate the peak positions for p-polarization (those are absent in s-polarization). The dashed lines represent the best fitted result to eq 2. These data were obtained at a molecular density of 0.08–0.10 nm\$^{-2}\$.

$$\frac{N_{\text{cis}}}{N_{\text{total}}} = 1 - e^{-\sigma_{\text{t}\rightarrow\text{c}} n_{\text{ph}}}, \quad \frac{N_{\text{trans}}}{N_{\text{total}}} = e^{-\sigma_{\text{t}\rightarrow\text{c}} n_{\text{ph}}} \quad (1)$$

where n_{ph} is the number of dosed photons per square centimeter. In the inset of Figure 2a, the normalized $\sigma_{\text{t}\rightarrow\text{c}}$ is plotted as a function of the incident laser power (P) at 405 and 446 nm excitation wavelengths. It is clear that $\sigma_{\text{t}\rightarrow\text{c}}$ remains constant with increasing power, thus indicating a linear power dependence of the tautomerization rate. Figure 2b shows $\ln\left(\frac{N_{\text{cis}}}{N_{\text{total}}}\right)$ versus n_{ph} plot at various excitation wavelengths. For all examined wavelengths, the evolution of $\frac{N_{\text{cis}}}{N_{\text{total}}}$ follows eq 1 and

ends up at a saturation of ~100%, proving the absence of the photoinduced backward cis → trans tautomerization.

Figure 2c displays the wavelength dependence of $\sigma_{\text{t}\rightarrow\text{c}}$ measured with p- and s-polarized light. For both polarizations, a steep increase is observed at a photon energy of ~2 eV, but $\sigma_{\text{t}\rightarrow\text{c}}$ for p-polarization is about twice as large as for s-polarization. The onset energy of 2 eV matches the energy of the Cu d-band edge, suggesting a substrate-mediated indirect excitation mechanism.³⁶ Hence, we attempted approximating the observed wavelength dependence of $\sigma_{\text{t}\rightarrow\text{c}}$ using a simple model that estimates the total number of hot carriers (N_{hc}) generated in the substrate through photon absorption,³⁷ given by

$$N_{\text{hc}} = N_{\text{ph}} A_{\text{p(s)}} \left\{ 1 - \exp\left(-\frac{\delta}{D}\right) \right\} \quad (2)$$

where N_{ph} is the number of photons, $A_{\text{p(s)}}$ the absorbance of bulk Cu at an incident angle of 65° for p- and s-polarized light, D the penetration depth of a photon into the Cu substrate, and δ the cutoff distance from which hot carriers can travel to the surface.³⁸ The dashed curves in Figure 2c represent the best fitted results, which qualitatively reproduce the general features of the experimental data; the fitted curve agrees rather well for s-polarization. Therefore, we concluded that the excitation process is dominated by an indirect mechanism mediated by hot carriers generated in the substrate. However, the agreement for p-polarization is not as good as for s-polarization, which may be due to narrow and broad peaks around 2.8 and 3.3–4.0 eV in the experimental data (indicated by the red arrows in Figure 2c). This deviation for p-polarization might be attributed to a minor contribution from direct photon absorption by the molecule–substrate complex.³⁹ Porphycene is known to exhibit intense Q and Soret bands around 1.9–2.4 and 3.2–3.8 eV, respectively, and also a very weak transition around 2.8–3.0 eV.²⁸ Hence, photons within these energy ranges could induce the direct excitation of the complex state. In this case, the observed differences between p- and s-polarization may be rationalized by the direction of the transition dipole moment and the relevant orbitals of the molecule–substrate complex.⁴⁰

Interestingly, the tautomerization cross section of porphycene in the visible–UV regime is much higher than that the other switching molecules observed on metal surfaces so far, for example, 10^{-23} – 10^{-22} cm 2 for azobenzene derivatives.^{4,14} This stark difference in the cross section is most likely due to the smaller activation barrier of tautomerization in porphycene, as the trans → cis tautomerization can be induced by STM with a threshold voltage of 170 mV (Figure 3b), compared to that of isomerization of azobenzene derivatives, as calculated to be 1.5–2.0 eV.^{41,42}

For further insight into the tautomerization process after photoexcitation, we investigated deuterated porphycene molecules in which the inner H atoms were substituted by deuterium (see inset of Figure 3a). Figure 3a shows an $\ln\left(\frac{N_{\text{cis}}}{N_{\text{total}}}\right)$ vs n_{ph} plot for light exposure at 532 nm, measured for h- and d-porphycene. $\sigma_{\text{t}\rightarrow\text{c}}$ is determined to be $1.3(\pm 0.1) \times 10^{-19}$ and $1.3(\pm 0.2) \times 10^{-21}$ cm 2 for h- and d-porphycene, respectively, hence revealing a remarkably strong isotope effect (~100). Note that the tautomerization rate of d-porphycene also shows a linear dependence on the incident laser power.

To identify the origin of the pronounced isotope effect, we investigated the STM-induced tautomerization (via an inelastic

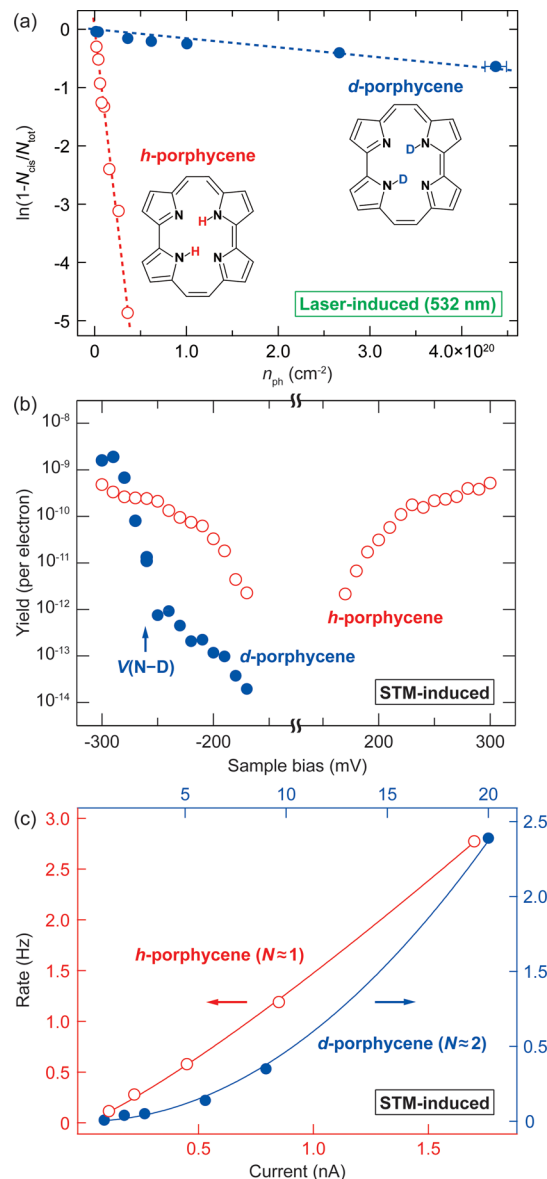


Figure 3. (a) $\ln\left(\frac{1 - N_{\text{cis}}}{N_{\text{tot}}}\right)$ versus n_{ph} plot at 532 nm excitation wavelength measured for *h*- and *d*-porphycene. The dashed lines represent the best fitted result to eq 1. (b) Voltage dependence of the STM-induced trans → cis tautomerization yield measured for *h*- (red circles) and *d*-porphycene (blue circles). (c) Current dependence of the STM-induced trans → cis tautomerization rate measured at $V_{\text{bias}} = -250$ and -230 mV for *h*- and *d*-porphycene, respectively. The experimental data were fitted to the power law ($R \propto I^N$). These data were obtained at a molecular density of 0.08 – 0.10 nm⁻².

electron tunneling process), which would be correlated with the photochemical reaction mediated by hot carriers. Figure 3b shows the voltage dependence of the trans → cis tautomerization yield measured for *h*- and *d*-porphycene. The observed threshold voltage of 170 mV is identical for both *h*- and *d*-porphycene, but the latter yield is smaller by about 2 orders of magnitude (100–360). Furthermore, the yield of *d*-porphycene shows a second steep increase with the onset voltage of ~260 mV, which nicely matches the energy of the N–D stretch.²¹ The threshold energy of ~170 meV is associated with low-frequency skeletal motions of porphycene.²¹ Figure 3c shows the current dependence of the trans → cis tautomerization rate

for *h*- and *d*-porphycene measured at $V_{\text{bias}} = -250$ and -230 mV, respectively, thus below the N–H(D) stretch excitation. An inelastic tunneling electron-induced adsorbate reaction follows the power law $R \propto I^N$ where R is the reaction rate, I is the tunneling current, and N is the reaction order.⁴³ Interestingly, the rates exhibit a nonlinear dependence on the current for *d*-porphycene, in contrast to a linear dependence for *h*-porphycene,⁴⁴ and N is found to be ~ 2 for *d*-porphycene,⁴⁵ indicating that tautomerization occurs via a two-electron process. This result indicates that tautomerization of *d*-porphycene requires more vibrational quanta of the skeletal mode than for *h*-porphycene, which is the reason why the tautomerization yield of *d*-porphycene is much lower than that of *h*-porphycene because such a multiple excitation is a less likely event. It should be noted that no backward cis → trans tautomerization was ever observed also in the STM-induced process.

Figure 4 summarizes the proposed mechanism of the photoinduced trans → cis tautomerization of porphycene on Cu(111). Figure 4a illustrates the energy diagram of porphycene and the Cu substrate. The molecule couples with the substrate and is expected to form molecule-induced states near the Fermi level. Because the tautomeric state is not stable (stationary) in a wide voltage range, we were unfortunately not able to measure scanning tunneling spectroscopy to characterize the electronic state of adsorbed porphycene. However, the long-range repulsive interaction between molecules, which is inferred from the adsorption behavior (Figure 1c), implies a charge transfer from the substrate to the molecule and (partial) filling of the lowest unoccupied molecular orbital near the Fermi level, as observed in free-base porphyrin on Ag(111).⁴⁶ Incoming photons are predominantly absorbed by the substrate and the hot carrier generation rate drastically increases above 2 eV because such photons can excite the high-density d-band electrons (I in Figure 4a). The generated hot carriers then attach to the molecule (II(e⁻) or II(h⁺) in Figure 4a), leading to a short-lived ionic state that subsequently returns to the neutral state by relaxation to the substrate (III in Figure 4). The attached carrier type and the involved orbitals are of fundamental importance in the process.⁴⁷ The hole attachment mechanism has been identified as a dominant process for switching of azobenzene derivatives on Au¹⁴ and Cu⁴⁸ surfaces when the d-band electrons are excited. This has been justified by the longer lifetime of hot holes than that of hot electrons.^{49–51} Additionally, with the photon energy close to the onset energy (~2 eV), hot electrons from the d-band edge should have a relatively low energy (a few hundred millielectronvolts), thus the amount of energy that is transferred to the adsorbate would be very limited. However, the threshold voltage of the trans → cis tautomerization was only ~170 meV in the STM-induced process (Figure 3b), suggesting that attachment of such low-energy electrons could also be an effective process in the present case. Accordingly, an unambiguous assignment of the carrier type and relevant orbitals remains an open question at this stage. This requires detailed understanding of the carrier dynamics and further insight could be provided by ultrafast spectroscopic studies like two-photon photoemission spectroscopy.

Figure 4b,c depicts a schematic energy diagram of the tautomerization process after photoexcitation. In the ground state ($S_0; \{\nu\} = 0$ where ν represents vibrational quanta), the trans configuration is thermodynamically stable, whereas the cis configuration is metastable. These states are separated by the

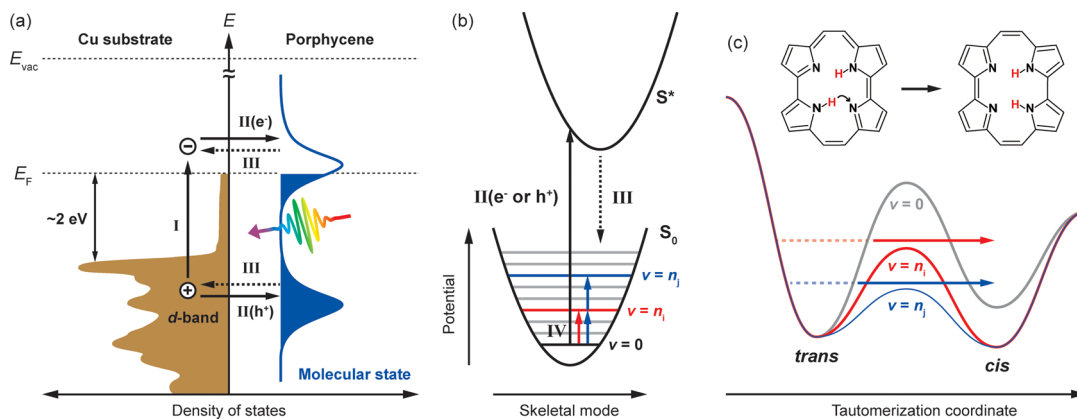


Figure 4. Proposed mechanism of the photoinduced trans → cis tautomerization of porphycene on Cu(111). (a) Energy diagram (density of states) of the Cu substrate (calculated⁵⁷) and porphycene (schematic). An incoming photon is absorbed either by a molecule–substrate complex, or by the substrate. The latter is the dominant process for the present case. The photon absorption is followed by hot carrier generation in the substrate (I), and the carriers then attach to the molecule (II). Subsequently, the attached carrier is relaxed to the substrate (III). (b,c) Schematic energy diagram of the tautomerization mechanism after photoexcitation. Upon the hot carrier attachment, the molecular vibration (skeletal modes) is excited after the Franck–Condon transition from the ground state (S_0 , $\{v\} = 0$) to the ionic state (S^*) and its de-excitation (indicated by black solid and dashed arrows). The excited skeletal modes promote the reaction through the reduction of the activation barrier. Different vibration quanta, n_i and n_j ($i < j$), are required to induce the reaction for h- and d-porphycene as depicted by red and blue lines (arrows), respectively, in (b). In the ground state, the trans configuration is thermodynamically stable, whereas the cis configuration might be more favorable in the vibrationally excited state. The dashed red and blue lines in (c) represent the zero-point energy for h- and d-porphycene, respectively. Note that the trans and cis configurations have a doubly degenerate state, but only one state is displayed for simplicity.

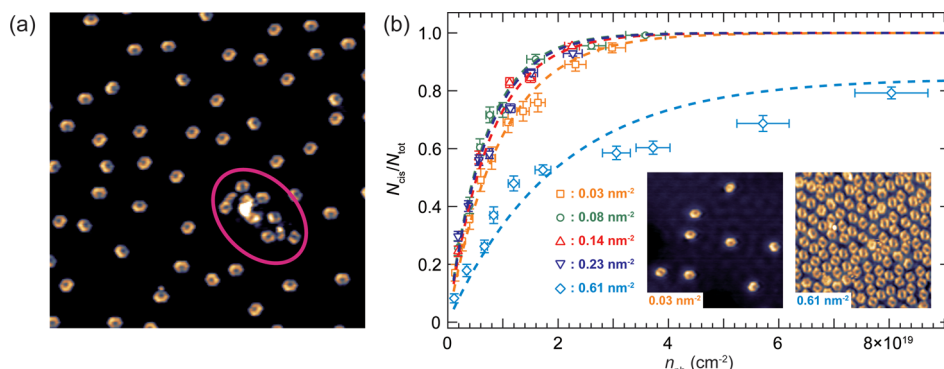


Figure 5. (a) STM image of porphycene molecules on Cu(111) including intrinsic surface defects (marked by red circle). The image was obtained after 14 h irradiation with a 780 nm diode laser with a photon flux density of $\sim 4.7 \times 10^{17} \text{ s}^{-1} \text{ cm}^{-2}$. Some of the molecules adjacent to the defect remain in the trans configuration. (b) $\frac{N_{\text{cis}}}{N_{\text{total}}}$ versus n_{ph} plot measured at 532 nm excitation wavelength and at various molecular densities. The dashed lines represent the best fitted results to eq 1. $\sigma_{t \rightarrow c}$ is determined to be $9.8 (\pm 0.2) \times 10^{-20}$, $1.34 (\pm 0.04) \times 10^{-19}$, $1.37 (\pm 0.05) \times 10^{-19}$, $1.22 (\pm 0.04) \times 10^{-19}$ and $3.43 (\pm 0.08) \times 10^{-20}$ at 0.03, 0.08, 0.14, 0.23, and 0.61 nm⁻², respectively. The inset shows typical STM images at a molecular density of 0.03 and 0.61 nm⁻².

activation barrier that cannot be overcome at 5 K (gray curve in Figure 4c). Upon the hot electron or hole attachment, the transition from the ground state to the ionic state (S^*) takes place. This transition is likely to occur so swiftly that nuclear motion is negligible during the excitation, thus following the Frack–Condon principle (solid arrow in Figure 4b). Subsequently, the ionic state is relaxed in a short time (dashed arrow in Figure 4b) via intramolecular vibrational relaxation, surface phonon and electron–hole pair excitation. The transient ionic state causes the electronic redistribution in the molecule, and the nuclear motion (molecular vibration) would follow this change (IV in Figure 4b) in the same manner as an inelastic electron tunneling process.⁵² For porphycene, fluorescence spectroscopy has revealed that the Frank–Condon transition accompanies the progression of the low-frequency skeletal modes.^{53–56} As discussed in the STM-induced process (Figure 3b), these vibration modes are associated with the trans

→ cis tautomerization on Cu(111). It is also known that a specific skeletal mode couples with the tautomerization coordinate and promotes the reaction through reduction of its activation barrier.^{53–56} Additionally, a comparable isotope effect (2 orders of magnitude) between the cross section (Figure 3a) and the yield of the inelastic electron-induced process (Figure 3b; below the N–D stretching energy) for h- and d-porphycene strongly suggests a crucial role of the skeletal mode excitation in the photoinduced process. In this case, the larger number of the vibrational quanta required for tautomerization in d-porphycene than for h-porphycene, which is proven by the current dependence of the STM-induced tautomerization rate (Figure 3c), could be attributed to their distinct zero-point energy in the reaction coordinate (as depicted by dashed lines in Figure 4c). Furthermore, the absence of the backward cis → trans tautomerization might imply that the cis configuration becomes more stable in the

vibrationally excited state due to the modulation of the potential energy landscape.

Finally, we demonstrate the local environmental impact on the photoinduced tautomerization. Figure 5a shows an STM image of porphycene molecules adjacent to intrinsic surface defects. As highlighted by the red circle, some of the molecules never switched, even after sufficiently long irradiation by which all of the other molecules on the clean terrace have reacted. In order to examine such a local environmental impact more systematically, we investigated tautomerization dynamics by varying molecular density (Figure 5b). At low densities ($0.03\text{--}0.23\text{ nm}^{-2}$), the molecules are well-separated from each other, and the reaction follows a first-order process. The cross section was determined to be $9.8 (\pm 0.2) \times 10^{-20}$, $1.34 (\pm 0.04) \times 10^{-19}$, $1.37 (\pm 0.05) \times 10^{-19}$, and $1.22 (\pm 0.04) \times 10^{-19}$ at 0.03 , 0.08 , 0.14 , and 0.23 nm^{-2} , respectively, for 532 nm excitation wavelength; thus the cross section appears to be slightly lower at 0.03 nm^{-2} (the difference is larger than the systematic error of $\sim 10\%$, see Supporting Information). A negligible difference for molecular densities at $0.08\text{--}0.23\text{ nm}^{-2}$ suggests that a long-range intermolecular interaction (e.g., dipole–dipole interaction) does not affect the tautomerization process in these regimes. However, the surface state of Cu(111) is expected to be influenced by molecular adsorption above a molecular density of $\sim 0.08\text{ nm}^{-2}$, as shown in our previous study.²³ This may cause changes in an optical absorption property of the substrate and/or hot carrier dynamics and consequently the subtle difference in the tautomerization cross section between 0.03 and $0.08\text{--}0.23\text{ nm}^{-2}$. On the other hand, the cross section substantially decreased at a higher molecular density (0.61 nm^{-2}), and the experimental data clearly deviated from a first-order process. Additionally, not all of the molecules were converted to the cis configuration, no matter how long they were subjected to irradiation. At this density, the intermolecular distances become much smaller and some of the molecules are in contact with each other as can be seen in the inset STM image of Figure 5b. In this situation, molecule–molecule interactions would play a critical role. Furthermore, the lack of a highly ordered molecular arrangement may cause subtly different local interactions and consequently different tautomerization behavior from molecule to molecule. This could be the reason why the evolution deviates from a first-order process. Additionally, the presence of unreacted molecules indicates quenching of tautomerization due to the intermolecular interaction.

In summary, we directly observed the photoinduced tautomerization of single porphycene molecules on the Cu(111) surface at 5 K by using a combination of the STM and laser excitation. It was found that the thermodynamically stable trans configuration can be unidirectionally converted to the metastable cis configuration by photoirradiation. The cross section exhibits a steep increase around 2 eV in the wavelength dependence and we demonstrated that the excitation process is governed by a substrate-mediated indirect mechanism. Combined with the voltage and current dependence of the inelastic tunneling electron-induced tautomerization with the STM, we proposed that the reaction occurs via vibrational excitation of skeletal modes after hot carrier attachment to the molecule and its relaxation. Furthermore, a pronounced isotope effect (~ 100) in the cross section pointed out a significant contribution from the zero-point energy in the reaction coordinate. Moreover, we demonstrated that the interaction between neighboring molecules or between a molecule and

intrinsic surface defects can strongly affect the tautomerization process. The observed cross section of $\sim 10^{-19}\text{ cm}^2$ in the visible–ultraviolet range was much higher than that of any other switching molecule on a metal surface observed so far. This efficient switching will open up the possibility of utilizing a photoactive molecular switch directly on metal electrodes.

Methods. All experiments were performed in an ultrahigh vacuum chamber (base pressure of $<10^{-10}\text{ mbar}$), equipped with a low-temperature STM (modified Omicron instrument with Nanonis Electronics). STM measurements were carried out at 5 K and all images were acquired in the constant-current mode. A Cu(111) surface was cleaned by repeated cycles of argon ion sputtering and annealing to $700\text{--}800\text{ K}$. The STM tip was made from a tungsten or gold wire. V_{bias} was applied to the sample. Porphycene molecules were deposited from a Knudsen cell (at an evaporation temperature of $450\text{--}500\text{ K}$). For photoirradiation, we used YAG lasers (266, 355 nm), diode lasers (405, 445.8, 532, and 780 nm), a HeNe laser (632.8 nm), and a tunable laser (a supercontinuum light source; 330–830 nm). The spectral bandwidth of the supercontinuum source can be tuned in the visible range and $6\text{--}8\text{ nm}$ was employed, while it is fixed to $<3\text{ nm}$ in the UV range. All other sources exhibit a bandwidth of $<1\text{ nm}$. The power range used is a few milliwatts for YAG, diode, and HeNe lasers, and a few tens of microwatts (in UV) to a few milliwatts (in visible–NIR) for the supercontinuum source. In order to avoid systematic errors caused by misalignment of the relative position between the STM and the beam spot, the lasers were shaped into a $2\text{--}3\text{ mm}$ top-hat square before coupling them to the STM junction (see Supporting Information). For very low-power UV light (330 and 380 nm with the supercontinuum source) and the 266 nm YAG laser, the beam was not shaped to the top-hat but a $2\text{--}3\text{ mm}$ Gaussian spot and the path was carefully aligned using a visible alignment laser.

■ ASSOCIATED CONTENT

§ Supporting Information

The Supporting Information is available free of charge on the ACS Publications website at DOI: [10.1021/acs.nanolett.5b04092](https://doi.org/10.1021/acs.nanolett.5b04092).

Chemical structure of the tautomeric states of porphycene and experimental details and data analysis. (PDF)

■ AUTHOR INFORMATION

Corresponding Author

*E-mail: kuma@fhi-berlin.mpg.de.

Present Address

(J.M.) BAM Bundesanstalt für Materialforschung und -prüfung, Berlin, Germany.

Notes

The authors declare no competing financial interest.

■ ACKNOWLEDGMENTS

H.B., S.L., J.M., L.G., M.W., and T.K. thank D. Baugh for valuable discussions, Y. Kumagai for helping the data analysis, and M. Krenz for technical support. T.K. acknowledges the support of Morino Foundation for Molecular Science. S.G. and J.W. acknowledge the support by the Polish National Science Center Grants DEC-2011/02/A/ST5/00043 and DEC-2013/10/M/ST4/00069.

■ REFERENCES

- (1) Feringa, B. L.; Browne, W. R. *Molecular Switches*; Wiley-VCH: Weinheim, Germany, 2011.
- (2) Browne, W. R.; Feringa, B. L. Light switching of molecules on surfaces. *Annu. Rev. Phys. Chem.* **2009**, *60*, 407–428.
- (3) Comstock, M. J.; Levy, N.; Kirakosian, A.; Cho, J.; Lauterwasser, F.; Harvey, J. H.; Strubbe, D. A.; Fréchet, J. M. J.; Trauner, D.; Louie, S. G.; Crommie, M. F. Reversible Photomechanical Switching of Individual Engineered Molecules at a Metallic Surface. *Phys. Rev. Lett.* **2007**, *99*, 038301.
- (4) Comstock, M. J.; Levy, N.; Cho, J.; Berbil-Bautista, L.; Crommie, M. F.; Poulsen, D. A.; Fréchet, M. J. Measuring reversible photomechanical switching rates for a molecule at a surface. *Appl. Phys. Lett.* **2008**, *92*, 123107.
- (5) Levy, M.; Comstock, M. J.; Cho, J.; Berbil-Bautista, L.; Kirakosian, A.; Lauterwasser, F.; Poulsen, D. A.; Fréchet, J. M. J.; Crommie, M. F. Self-Patterned Molecular Photoswitching in Nano-scale Surface Assemblies. *Nano Lett.* **2009**, *9*, 935–939.
- (6) Comstock, M. J.; Strubbe, D. A.; Berbil-Bautista, L.; Levy, N.; Cho, J.; Poulsen, D.; Fréchet, J. M. J.; Louie, S. G.; Crommie, M. F. Determination of Photoswitching Dynamics through Chiral Mapping of Single Molecules Using a Scanning Tunneling Microscope. *Phys. Rev. Lett.* **2010**, *104*, 178301.
- (7) Bazarnik, M.; Henzl, J.; Czajka, R.; Morgenstern, K. Light driven reactions of single physisorbed azobenzenes. *Chem. Commun.* **2011**, *47*, 7764–7766.
- (8) Henzl, J.; Puschning, P.; Ambrosch-Draxl, C.; Schaate, A.; Ufer, B.; Behrens, P.; Morgenstern, K. Photoisomerization for a molecular switch in contact with a surface. *Phys. Rev. B: Condens. Matter Mater. Phys.* **2012**, *85*, 035410.
- (9) Bazarnik, M.; Jurczyszyn, L.; Czajka, R.; Morgenstern, K. Mechanism of a molecular photo-switch adsorbed on Si(100). *Phys. Chem. Chem. Phys.* **2015**, *17*, 5366–5371.
- (10) Bronner, C.; Schulze, G.; Franke, K. J.; Pascual, J. I.; Tegeder, P. Switching ability of nitro-spiropyran on Au(111): electronic structure changes as a sensitive probe during a ring-opening reaction. *J. Phys.: Condens. Matter* **2011**, *23*, 484005.
- (11) Schulze, G.; Franke, K. J.; Pascual, J. I. Induction of a Photostationary Ring-Opening—Ring-Closing State of Spiropyran Monolayers on the Semimetallic Bi(110) Surface. *Phys. Rev. Lett.* **2012**, *109*, 026102.
- (12) Alemani, M.; Selvanathan, S.; Ample, F.; Peters, M. V.; Rieder, K.-H.; Moresco, F.; Joachim, C.; Hecht, S.; Grill, L. Adsorption and Switching Properties of Azobenzene Derivatives on Different Noble Metal Surfaces: Au(111), Cu(111), and Au(100). *J. Phys. Chem. C* **2008**, *112*, 10509–10514.
- (13) Dri, C.; Peters, M. V.; Schwarz, J.; Hecht, S.; Grill, L. Spatial periodicity in molecular switching. *Nat. Nanotechnol.* **2008**, *3*, 649–653.
- (14) Wolf, M.; Tegeder, P. Reversible molecular switching at a metal surface: A case study of tetra-tert-butyl-azobenzene on Au(111). *Surf. Sci.* **2009**, *603*, 1506–1517.
- (15) Gahl, C.; Ishioka, K.; Zhong, Q.; Hotzel, A.; Wolf, M. Structure and dynamics of excited electronic states at the adsorbate/metal interface: $C_6F_6/Cu(111)$. *Faraday Discuss.* **2000**, *117*, 191–202.
- (16) Yang, A.; Shipman, S. T.; Garrett-Roe, S.; Johns, J.; Strader, M.; Szymanski, P.; Muller, E.; Harris, C. Two-Photon Photoemission of Ultrathin Film PTCDA Morphologies on Ag(111). *J. Phys. Chem. C* **2008**, *112*, 2506–2513.
- (17) Bronner, C.; Priewisch, B.; Rück-Braun, K.; Tegeder, P. Photoisomerization of an Azobenzene on the Bi(111) Surface. *J. Phys. Chem. C* **2013**, *117*, 27031–27038.
- (18) Auwärter, W.; Écija, D.; Klappenberg, F.; Barth, J. V. Porphyrins at interfaces. *Nat. Chem.* **2015**, *7*, 105–120.
- (19) Liljeroth, P.; Repp, J.; Meyer, G. Current-Induced Hydrogen Tautomerization and Conductance Switching of Naphthalocyanine Molecules. *Science* **2007**, *317*, 1203–1206.
- (20) Auwärter, W.; Seufert, K.; Bischoff, F.; Ecija, D.; Vijayaraghavan, S.; Joshi, S.; Klappenberg, F.; Samudrala, N.; Barth, J. V. A surface-anchored molecular four-level conductance switch based on single proton transfer. *Nat. Nanotechnol.* **2011**, *7*, 41–46.
- (21) Kumagai, T.; Hanke, F.; Gawinkowski, S.; Sharp, J.; Kotsis, K.; Waluk, J.; Persson, M.; Grill, L. Thermally and vibrationally induced tautomerization of single porphycene molecules on a Cu(110) surface. *Phys. Rev. Lett.* **2013**, *111*, 246101.
- (22) Kumagai, T.; Hanke, F.; Gawinkowski, S.; Sharp, J.; Kotsis, K.; Waluk, J.; Persson, M.; Grill, L. Controlling intramolecular hydrogen transfer in a porphycene molecule with single atoms or molecules located nearby. *Nat. Chem.* **2013**, *6*, 41–46.
- (23) Ladenthin, J. N.; Grill, L.; Gawinkowski, S.; Waluk, J.; Kumagai, T. Hot carrier-induced tautomerization within a single porphycene molecule on Cu(111). *ACS Nano* **2015**, *9*, 7287–7295.
- (24) Kumagai, T. Direct observation and control of hydrogen-bond dynamics using low-temperature scanning tunneling microscopy. *Prog. Surf. Sci.* **2015**, *90*, 239–291.
- (25) Vogel, E.; Köcher, M.; Schmickler, H.; Lex, J. Porphycene—a novel porphin isomer. *Angew. Chem., Int. Ed. Engl.* **1986**, *25*, 257–259.
- (26) Gawinkowski, S.; Walewski, Ł.; Vdovin, A.; Slenczka, A.; Rols, S.; Johnson, M. R.; Lesyng, B.; Waluk, J. Vibrations and hydrogen bonding in porphycene. *Phys. Chem. Chem. Phys.* **2012**, *14*, 5489–5503.
- (27) Fita, P.; Urbańska, N.; Radzewicz, C.; Waluk, J. Ground- and excited-state tautomerization rates in porphycenes. *Chem. - Eur. J.* **2009**, *15*, 4851–4856.
- (28) Waluk, J.; Müller, M.; Swiderek, P.; Köcher, M.; Vogel, E.; Hohlneicher, G.; Michl, J. Electronic states of porphycenes. *J. Am. Chem. Soc.* **1991**, *113*, 5511–5527.
- (29) Piwoński, H.; Stupperich, C.; Hartschuh, A.; Sepiol, J.; Meixner, A.; Waluk, J. Imaging of Tautomerism in a Single Molecule. *J. Am. Chem. Soc.* **2005**, *127*, 5302–5303.
- (30) Piwoński, H.; Hartschuh, A.; Urbańska, N.; Pietraszkiewicz, M.; Sepiol, J.; Meixner, A. J.; Waluk, J. Polarized Spectroscopy Studies of Single Molecules of Porphycenes: Tautomerism and Orientation. *J. Phys. Chem. C* **2009**, *113*, 11514–11519.
- (31) Zhou, X.-L.; Zhu, X.-Y.; White, J. M. Photochemistry at adsorbate/metal interfaces. *Surf. Sci. Rep.* **1991**, *13*, 73–220.
- (32) Zimmermann, F. M.; Ho, W. State resolved studies of photochemical dynamics at surfaces. *Surf. Sci. Rep.* **1995**, *22*, 127–247.
- (33) Guo, H.; Saalfrank, P.; Seideman, T. Theory of photoinduced surface reactions of admolecules. *Prog. Surf. Sci.* **1999**, *62*, 239–303.
- (34) Yates, J. T., Jr.; Petek, H. Introduction: Photochemistry and Photophysics on Surfaces. *Chem. Rev.* **2006**, *106*, 4113–4115.
- (35) Matsumoto, Y. Photochemistry and Photo-Induced Ultrafast Dynamics at Metal Surfaces. *Bull. Chem. Soc. Jpn.* **2007**, *80*, 842–855.
- (36) Heimann, P.; Hermanson, J.; Miosga, H.; Neddermeyer, H. d-like surface-state bands on Cu(100) and Cu(111) observed in angle-resolved photoemission spectroscopy. *Phys. Rev. B: Condens. Matter Mater. Phys.* **1979**, *20*, 3059–3066.
- (37) Ying, Z. C.; Ho, W. Thermoinduced and photoinduced reactions of NO on Si(111) 7×7 . III. Photoreaction mechanisms. *J. Chem. Phys.* **1990**, *93*, 9089–9095.
- (38) The value of δ is estimated to be the order of 10 nm, provided a lifetime of 10 fs and speed of 10^6 m/s for carriers. The skin depth $D = \lambda/(2\pi k)$ is derived from the incident wavelength λ and the extinction coefficient of copper.
- (39) Ying, Z. C.; Ho, W. Alkali promotion of photodissociation of adsorbed $Mo(CO)_6$. *Phys. Rev. Lett.* **1990**, *65*, 741–744.
- (40) Wolf, M.; Hotzel, A.; Knoesel, E.; Velic, D. Direct and indirect excitation mechanisms in two-photon photoemission spectroscopy of Cu(111) and CO/Cu(111). *Phys. Rev. B: Condens. Matter Mater. Phys.* **1999**, *59*, 5926–5935.
- (41) Füchsel, G.; Klamroth, T.; Dokic, J.; Saalfrank, P. On the Electronic Structure of Neutral and Ionic Azobenzenes and Their Possible Role as Surface Mounted Molecular Switches. *J. Phys. Chem. B* **2006**, *110*, 16337–16345.

- (42) Maurer, R. J.; Reuter, K. Bistability Loss as a Key Feature in Azobenzene (Non-)Switching on Metal Surfaces. *Angew. Chem.* **2012**, *124*, 12175–12177.
- (43) Stipe, B. C.; Rezaei, M. A.; Ho, W.; Gao, S.; Persson, M.; Lundqvist, B. I. Single-Molecule Dissociation by Tunneling Electrons. *Phys. Rev. Lett.* **1997**, *78*, 4410.
- (44) A linear dependence of the rates was also observed at $V_{\text{bias}} = 200$ mV for *h*-porphycene.
- (45) The rates of *d*-porphycene show a linear dependence on the current at a voltage above the N–D stretching excitation (~ 260 meV), indicating that the N–D stretching can excite the required vibrational quanta of the skeletal mode in one step via intramolecular vibrational relaxation.
- (46) Bischoff, F.; Seufert, K.; Auwäter, W.; Joshi, S.; Vijayaraghavan, S.; Ecija, D.; Diller, K.; Papageorgiou, A. C.; Fischer, S.; Allegretti, F.; Duncan, D. A.; Klappenberger, F.; Blobner, F.; Han, R.; Barth, J. V. How Surface Bonding and Repulsive Interactions Cause Phase Transformations: Ordering of a Prototype Macroyclic Compound on Ag(111). *ACS Nano* **2013**, *7*, 3139–3149.
- (47) Petek, H. Photoexcitation of adsorbates on metal surfaces: One-step or three-step. *J. Chem. Phys.* **2012**, *137*, 091704.
- (48) García, N.; Arnolds, H. Hot hole-induced dissociation of NO dimers on a copper surface. *J. Chem. Phys.* **2011**, *135*, 224708.
- (49) Knoesel, E.; Hotzel, A.; Wolf, M. Ultrafast dynamics of hot electrons and holes in copper: Excitation, energy relaxation, and transport effects. *Phys. Rev. B: Condens. Matter Mater. Phys.* **1998**, *57*, 12812.
- (50) Petek, H.; Nagano, H.; Ogawa, S. Hole Decoherence of d Bands in Copper. *Phys. Rev. Lett.* **1999**, *83*, 832.
- (51) Gerlach, A.; Berge, K.; Goldmann, A.; Campillo, I.; Rubio, A.; Pitarke, J. M.; Echenique, P. M. Lifetime of d holes at Cu surfaces: Theory and experiment. *Phys. Rev. B: Condens. Matter Mater. Phys.* **2001**, *64*, 085423.
- (52) Persson, B. N. J.; Baratoff, A. Inelastic electron tunneling from a metal tip: The contribution from resonant processes. *Phys. Rev. Lett.* **1987**, *59*, 339.
- (53) Mengesha, E. T.; Sepiol, J.; Borowicz, P.; Waluk, J. Vibrations of porphycene in the S_0 and S_1 electronic states: Single vibronic level dispersed fluorescence study in a supersonic jet. *J. Chem. Phys.* **2013**, *138*, 174201.
- (54) Gil, M.; Waluk, J. Vibrational Gating of Double Hydrogen Tunneling in Porphycene. *J. Am. Chem. Soc.* **2007**, *129*, 1335–1341.
- (55) Mengesha, E. T.; Zehnacker-Rentien, A.; Sepiol, J.; Kijak, M.; Waluk, J. Spectroscopic Study of Jet-Cooled Deuterated Porphycenes: Unusual Isotopic Effects on Proton Tunneling. *J. Phys. Chem. B* **2015**, *119*, 2193–2203.
- (56) Vdovin, A.; Waluk, J.; Dick, B.; Slenczka, A. Mode-selective promotion and isotope effects of concerted double-hydrogen tunneling in porphycene embedded in superfluid helium nanodroplets. *ChemPhysChem* **2009**, *10*, 761–765.
- (57) Tsymbal, E. Y.; Pettifor, D. Perspectives of giant magnetoresistance. *Solid State Phys.* **2001**, *56*, 113–237.